

## Stress Distribution in Ion Exchanged Glass

**E.E. Shaisha, A.A. Bahgat and S.H. Salah**

*Department of Physics, Faculty of Science, Al-Azhar University, Nasr City, Cairo, Egypt*

---

**ABSTRACT:** Experimental stress distribution for the forward ion exchange at two different temperatures 350°C and 500°C, obtained by successive slicing and photoelastic measurements, confirms the profiles calculated from the analogy to thermal stress theory and from finite element stress analysis. The measured profiles for the reverse field cases show much lower stresses than those predicted by the same theory. A theoretical analysis for the stress distribution calculated from the analogy to the thermal stress distribution and the effect of sample distortion due to slicing are briefly discussed.

It was known, at least since the time of Griffith (1920), that the low strength of glass was due to stress concentration at the tip of microcracks present on the glass surface. Under tensile stresses these cracks grow slowly by a stress corrosion mechanism (Wiederhorn 1975) leading to fracture at much lower stress than the instantaneous fracture strength. On the other hand, flow free glass specimens show a tensile fracture strength of  $10^4$  MN/m<sup>2</sup> (Holloway 1973), or ~ 10 times that of steel. It, therefore, became important to protect the surface of the glass by development of a residual compressive stress layer on the glass surface. Such a layer could be produced by thermal tempering (Wiederhorn 1975), cladding a higher with a lower expansion coefficient glass (Krohn and Cooper 1969), by ion exchange above the stress relaxation temperature such that a layer is formed on the glass surface which has lower expansion coefficient than the glass bulk (Hood and Stookey 1964), or by ion exchange of larger for smaller ions below the stress relaxation temperature. An ion exchanged glass, in principle, should have a strength 3-10 times that of a tempered glass. Besides strengthening of glass articles, the ion exchange process has been used to develop the refractive index gradient for optical

waveguides and to improve the corrosion resistance of the glass. Therefore, it is very important to study the stress distribution arising from ion exchange in the glass which is the purpose of this paper.

Richmond *et al.* (1964) recognized that the stress due to the presence of concentration differences in the material are analogous to those produced by temperature differences. Cooper and Krohn (1969) found that ion exchange stresses in glass fiber are consistent with the predicted stresses from analogy to thermal stresses with a dilation coefficient  $B = 2.8 \times 10^{-4}/\text{wt fraction } K^+$ . Ohta and Hara (1970) utilized the analogy to thermal stress to calculate the stresses in soda lime glass plates after ion exchange with the application of a single electric field. They found that calculated intrinsic residual stresses gave uniform compression in the exchanged layer balanced by tension in the rest of the glass. Sane and Cooper (1978) have shown that slicing an exchanged specimen changes its stress state. In particular, that the anomalous tension minima reported by Schaeffer and Heinze (1974) is introduced by taking a slice from the treated plate.

In the present contribution, the residual stress distribution was determined for an ion exchanged soda lime glass tubes after slicing. The measurements were done in glass tubes which were ion exchanged at 350°C and 500°C to predict the stress relaxation and the dependence on slice thickness due to elastic deformation after slicing. The experimental stress distribution is compared with that obtained from the solution of the elastic equations and the finite element analysis fitted by a computer program.

### Theoretical Treatment

#### 1. A Solution of Stresses from the Thermal Stress Theory

By analogy to thermal stress theory, the stress distribution can be determined by replacing temperature differences by concentration differences and the thermal expansion coefficient by the dilation coefficient. Consider an ion exchanged tube of two radii  $a$  and  $b$  as shown in Fig. 1-a. For plane strain (appropriate for long tubes) with concentration variation across the radial direction only, the following solution for the stress equations can be obtained (Abou-El-Leil and Cooper 1978) at the outer exchanged layer.

Stress	$a < r < b - \Delta$ (tension)	$b - \Delta < r < b$ (compression)	
Axial $\sigma_{zz}$	$\frac{2b\Delta k_0}{(b^2 - a^2)}$	$-K_0$	
Radial $\sigma_{rr}$	$\frac{b\Delta K_0}{(b^2 - a^2)} \left[ 1 - \left(\frac{a}{r}\right)^2 \right]$	$\frac{K_0}{2} \left[ \left(\frac{b}{r}\right)^2 - 1 \right]$	(1)
Tangential $\sigma_{\theta\theta}$	$\frac{b\Delta K_0}{(b^2 - a^2)} \left[ 1 + \left(\frac{a}{r}\right)^2 \right]$	$\frac{-K_0}{2} \left[ \left(\frac{b}{r}\right)^2 + 1 \right]$	

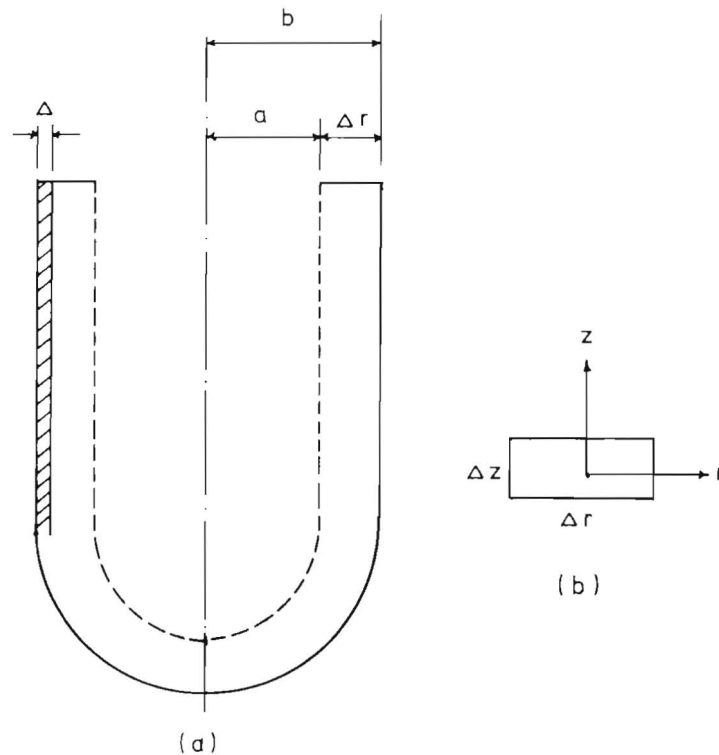


**Fig. 1-a.** Geometry of a tube exchanged from outside surface.  
**b.** A sliced beam.

Where  $b$  &  $a$  are the tube outside and inside radii respectively,  $K_0 = \frac{BEC_0}{(1-\nu)}$  which is numerically equal to  $\sigma_{zz}$  in the exchanged layer,  $\Delta \ll \frac{b-a}{2}$ , where  $\Delta$  is the ion exchange depth,  $E$  is the modulus of elasticity (Young's modulus)  $\nu$  is the Poisson's ratio and  $\sigma_{zz} = \sigma_{\theta\theta} + \sigma_{rr}$ .

## 2. The Finite Element Stress Analysis Under the Generalized Plane Strain Condition

A two dimensional isoparametric finite element program was available to perform the analysis of a thermal or compositional stress problem under plane stress or plane strain condition. Node points were selected by dividing the  $rz$  plane into rectangular elements which were purposely smaller near the boundaries. Using the physical properties and the composition distribution (in mol. fraction)

$$C(r,t) = C(r) \operatorname{erfc} \left( \frac{\Delta r - r}{2\sqrt{Dt}} \right) \dots\dots (2)$$

where  $C(r)$  is the steady surface concentration of the exchanged ion,  $\Delta r = b - a$ ,  $D$  is the interdiffusion coefficient (assumed constant) and  $t$  is the ion exchange time. The computer program systematically adjusts the stresses on the lines between the nodes so as to minimize the strain energy and to satisfy the boundary conditions of (a) no displacement in the  $z$ -direction of nodes on the  $r$ -axis (radius of the cylinder), (b) no displacements in the  $r$ -direction of the nodes of the  $z$ -axis of symmetry and (c) zero normal stress on the surface planes  $r = \frac{\Delta r}{2}$  and  $z = \frac{\Delta z}{2}$  (Assuming a beam of width  $\Delta z$  is sliced from the cylinder as shown in Fig. 1-b). In input parameters (Schaeffer and Heinze 1974) used were the product of dilation coefficient  $B$  and surface concentration  $C(r)$ , *i.e.*  $BC(r) = 24 \cdot 10^{-4}$ ,  $E = 700,000$   $\text{kg/cm}^2$ , and  $\nu = 0.28$ . The output gave stresses in each element and the displacement of each node.

### 3. Effect of Slicing

A detailed analysis of this effect was given by Sane and Cooper (1978). Their results showed that to minimize an error in the measurements of compressive stresses, the slice thickness  $\delta z$  must satisfy either of the following conditions.

$$\text{or } \left. \begin{array}{l} \delta z \leq 2\sqrt{Dt} \\ \delta z \gg \Delta x \end{array} \right\} \dots\dots\dots (3)$$

where  $D$  is the interdiffusion coefficient,  $t$  is the time of ion exchange and  $\Delta x$  is the thickness of the beam which was sliced from an ion exchanged slab.

### Stress Measurements

The middle portion of the exchanged tubes was sliced and ground using 400-grit SiC paper and then polished with diamond compound. Optical retardation was determined by reading a Berek compensator using a polarizing microscope; it was then converted into the stress difference ( $\sigma_{\theta\theta} - \sigma_{rr}$ ) using the appropriate stress optical coefficient  $26 \cdot 10^{-7}$   $\text{MN/m}^2$  for Soda lime glass used\*. Some adjustments were made in the polarizing microscope to make of the principal stresses parallel to either the polarizer or the analyzer and the other principal stress had a direction normal to the first. The compressive stress was measured after rotating the specimen by an angle of  $90^\circ$  to the direction of the tensile stress. Equation (1) shows that ( $\sigma_{\theta\theta} - \sigma_{rr}$ ) is negative for the compressive stress and +ve for the tensile stress. This means that the sign of the compressive stress is always opposite to that of the tensile stress. In general,  $\sigma_{\theta\theta} \gg \sigma_{rr}$  because the radius of the glass tube is sufficiently large compared to the thickness of the exchanged layer. The finite element stress analysis (FESA) was carried out assuming a constant concentration and gradient concentration.

\* Owens - Illinois Inc catil ge, vinceland, N.H. U.S.A.

To estimate the precision of measurements, optical retardation was measured at different points at the same radius of a given sample. The results showed that twice the standard deviation was invariably  $< 10\%$  of the reading. When necessary, tilt of the cylindrical axis of the sample with respect to the microscope axis was minimized by using a universal stage.

### Results and Discussion

Photoelastic measurement of the ion exchanged samples at  $350^\circ\text{C}$  and  $500^\circ\text{C}$  showed the stress dependence on slice thickness,  $h$ , as reported previously (Abou-El-leil and Cooper 1978) due to elastic deformation after slicing (Sane and Cooper 1978). The stress distribution for thin ( $h = 100\ \mu\text{m}$ ) and thick ( $h = 1000\ \mu\text{m}$ ) sliced rings are shown in Fig. 2 and Fig. 3, respectively. The experimental results at the above temperatures are compared with that obtained using FESA as marked on the figures.

The results show that in the case of the thin ring Fig. 2, the maximum stress at the edge of the exchange temperature  $350^\circ\text{C}$  is equal to that obtained using the FESA (about  $1050\ \text{MN/m}^2$ ) whereas it is about  $450\ \text{MN/m}^2$  at  $500^\circ\text{C}$ .

The low value of the stress obtained at  $500^\circ\text{C}$  was attributed to the viscoelastic relaxation (Shaisha and Cooper 1981).

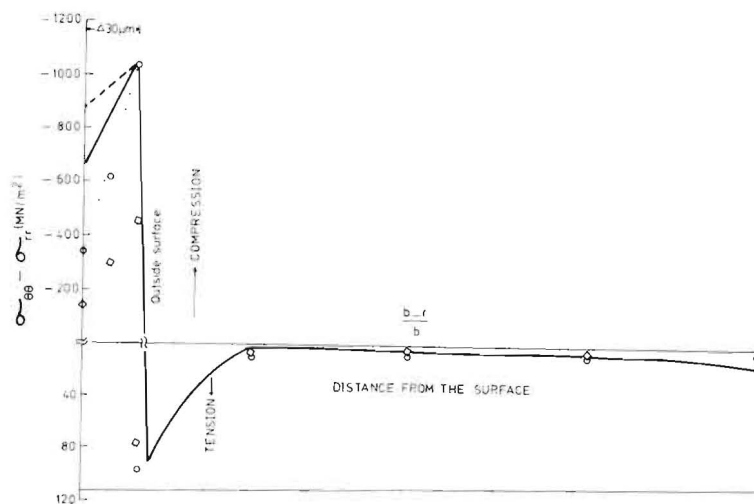


**Fig. 2.** Stress distribution for thin ring [ $h = 100\ \mu\text{m}$ ]

- At  $350^\circ\text{C}$
- At  $500^\circ\text{C}$
- Finite element analysis (variable  $\text{K}^+$  concentration)
- Finite element analysis (constant  $\text{K}^+$  concentration)

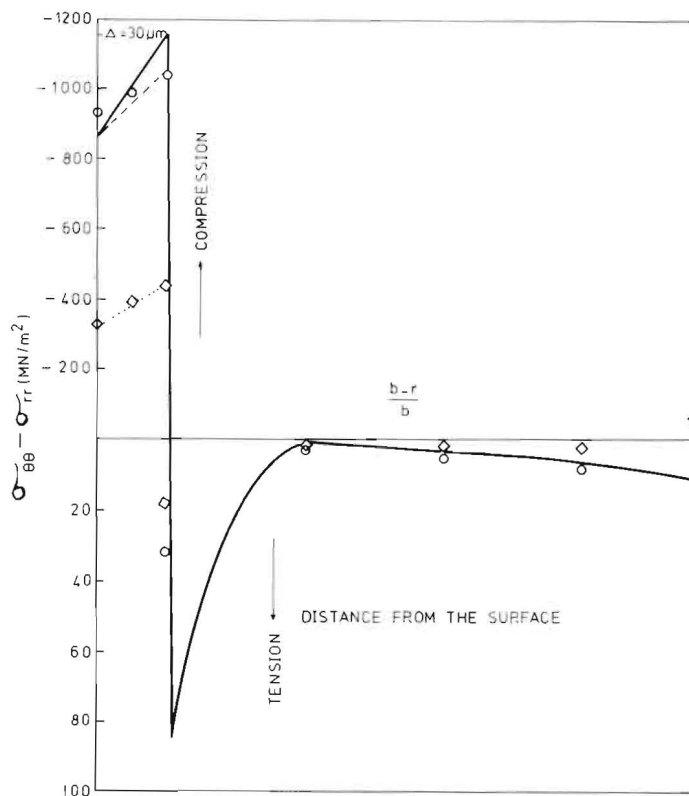


**Fig. 3.** Stress distribution for thick ring ( $h = 1000 \mu\text{m}$ )

- At 350°C
- At 500°C
- Finite element analysis (variable  $K^+$  concentration)
- Finite element analysis (constant  $K^+$  concentration)

Assuming the compressive stress at the surface of the exchanged layer is  $\sigma$  and that at its edge is  $\sigma_{\max}$ , it was found that the values of the reduced stress ( $\sigma/\sigma_{\max}$ ) is equal to 0.33 for the experimental results at the temperatures 350°C and 500°C. The reduced stress values obtained by FESA were found to be 0.62 (concentration of potassium ions assumed to be 20% of that at the edge) and 0.84 for constant concentration of  $K^+$  ions; see Fig. 2 for the case of thin ring. Those values obtained for the case of thick ring in Fig. 3 are 0.88 (350°C), 0.75 (500°C), 0.75 (FESA with variation of concentration) and 0.95 (FESA with constant concentration). The stress build up due to the concentration differences in the material was recognized by Richmond *et al.* (1964). For long tubes with concentration variation along the radial direction, the axial stress is given by (Abou-El-leil and Cooper 1978)

$$\sigma_{zz} = \sigma_{\theta\theta} + \sigma_{rr} = \frac{BE}{(1-\nu)} \left\{ \left[ \frac{2}{(b^2 - a^2)} \right] \int_a^b crdr - c \right\} \quad (4)$$

where the equation's parameters have the same definition mentioned above. This equation shows the concentration difference (between  $K^+$  ions and  $Na^+$  ions) dependence of the stress. Since the size of  $K^+$  ions (radius 1.33 Å) is greater than that of  $Na^+$  ions (radius 0.98 Å), the structure would tend to expand in all directions to accommodate larger  $K^+$  ions. This expansion along the axial direction of the cylindrical tube (along the z-direction) is prevented by the unexchanged part of the glass due to the plane strain condition. This phenomenon gives compressive stresses ( $\sigma_{\theta\theta}$  and  $\sigma_{zz}$ ) in the exchanged layer which is balanced by a tensile stress in the unexchanged part of the glass. The expansion of the network can be instantaneous (Elastic), time dependent (Viscous), or both (Viscoelastic). The last two depend on the temperature.

The faster relaxation than the predicted one near the surface of the exchanged layer could arise from:

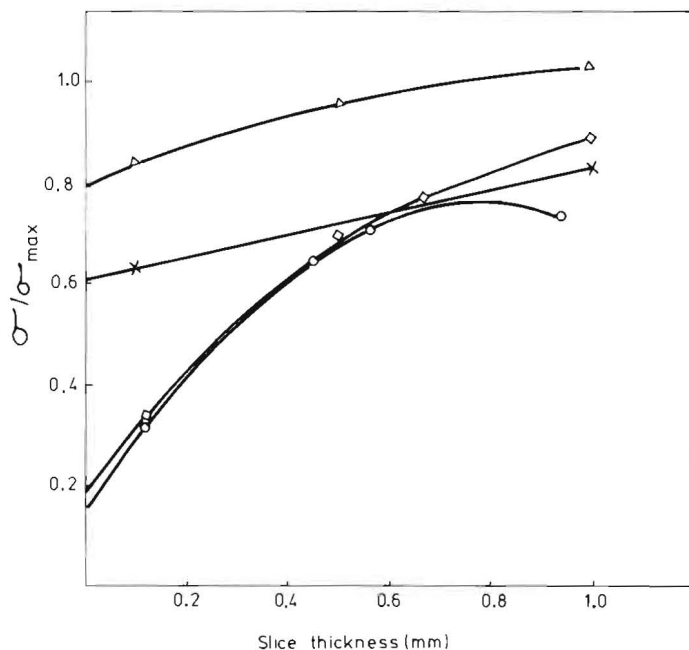


**Fig. 4.** Effect of slicing on the stress  
 □ At 350°C  
 ○ At 500°C  
 △ Finite element analysis (constant  $K^+$  concentration)  
 × Finite element analysis (variable  $K^+$  concentration)

(i) The dependence of the concentration on the relaxation time

(ii) The concentration gradient of potassium ions within the exchanged layer. This is indicated by Fig. 2 and Fig. 3 which show the comparison between the results obtained by FESA assuming a variation in the concentration and that assuming a constant concentration, and

(iii) a sample distortion due to slicing which is very clear in the case of a thin ring.

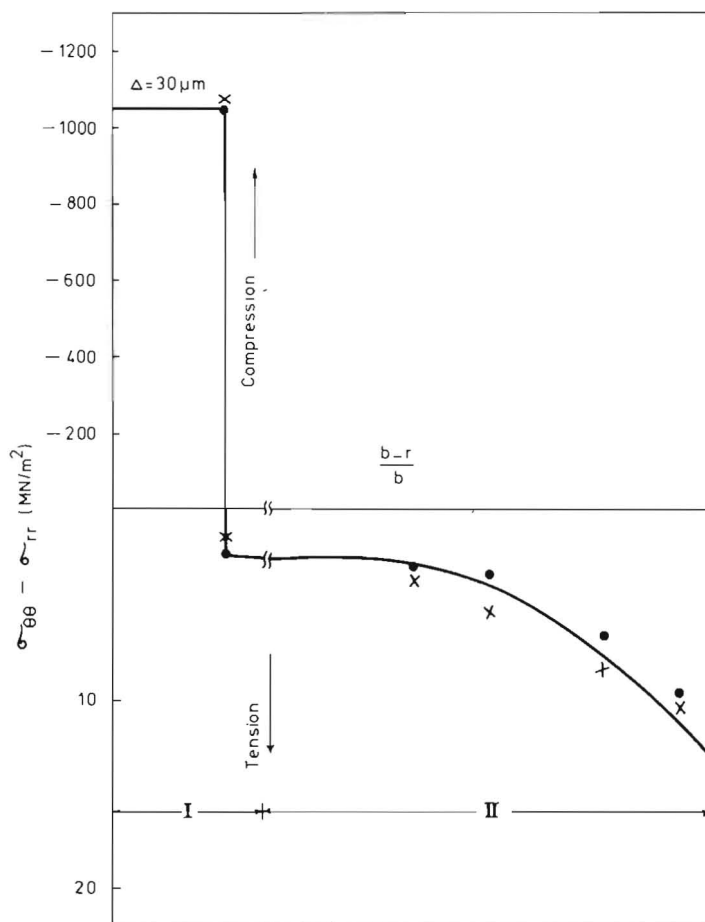


**Fig. 5.** Distribution of Principal stress difference in tube (ion exchange on outside surface).

— Theoretical (elastic equation 1)

● Experimental

× Finite element analysis.

Range I Thickness of the exchanged layer (compression layer) in  $\mu\text{m}$

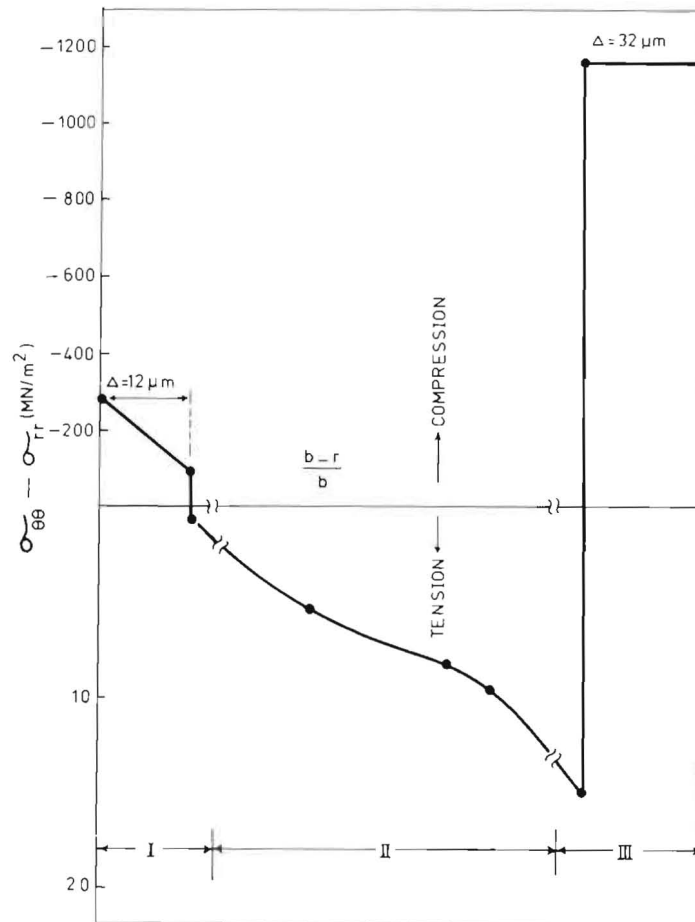
Range II Thickness of the glass bulk (Tension region).



Figure 4 shows that the reduced stress increases with the increase of the ring thickness as indicated by the experimental curves at 350°C and 500°C and is almost unity for the long tubes. The results obtained in Fig. 4 show that to minimize an error in the measurements of compressive stresses, the slice thickness,  $h$ , must satisfy the condition

$$h \gg \Delta r$$

where  $\Delta r = b - a$  is the thickness of the glass tube. This result is in a good



**Fig. 6.** Distribution of principal stress difference in a tube (ion exchange on the outside and inside surfaces) double exchange.

Range I Thickness of the exchanged layer (compression layer) on the outside surface in  $\mu\text{m}$ .

Range II Thickness of the glass bulk (tension region).

Range III Thickness of the exchanged layer (compression layer) on the inside surface in  $\mu\text{m}$ .

agreement with that obtained by Sane and Cooper (1978) for the change of stress state due to the elastic deformation after slicing.

The principal stress difference distribution obtained by extrapolating all the results including those in Fig. 2 and Fig. 3, to infinite thickness  $1/h = 0$  is compared in Fig. 5 with the corresponding principal stress difference ( $\sigma_{\theta\theta} - \sigma_{rr}$ ), calculated from eqn (1) by substituting  $K_0 = 1050 \text{ MN/m}^2$  (this value corresponding to the maximum, axial stress at  $350^\circ\text{C}$ ), and that obtained from the FESA. The close agreement confirms that the stress state in the unsliced tubes is essentially predicted by eqn (1). It should be noted here that  $\sigma_{\theta\theta}(\text{unsliced tube}) = \frac{\sigma_{\theta\theta}(\text{ring})}{1 - \nu}$  and  $\sigma_{rr}(\text{unsliced tube}) = \frac{\sigma_{rr}(\text{ring})}{1 - \nu}$ , where  $\nu$  is the poisson's ratio, therefore the axial stress  $\sigma_{zz}$  of the unsliced tube could be determined.

In Fig. 6, the stress difference ( $\sigma_{\theta\theta} - \sigma_{rr}$ ) was measured for a doubly ion exchanged layer at  $350^\circ\text{C}$  (the mechanism of doubly ion exchange is explained elsewhere (Shaisha and Bahgat 1984)).

The maximum stress at the double exchanged layer is much lower than that of the single exchange one (inside surface). The fast stress relaxation in the doubly exchanged layer could be interpreted as due to the decrease in the potassium concentration in the doubly exchanged layer (Abou-Eil-Leil and Cooper 1979). Also, the integrated flux was equal in both directions so that the composition near the outer surface did not return to its original state.

### Conclusion

In the case of single ion exchange, the maximum compressive and tensile stresses measured for the slice rings (Plane stress) are obtained around the boundary of the exchanged layer, whilst they are minimum near the surface. The compressive stress which is obtained in an ion exchanged glass after reversing the direction of the applied electric field (doubly ion exchanged layer) is much lower than the values predicted from the analogy of thermal stress theory. Slicing of the glass tube changes its stress state. A good agreement between the experimental stress distribution and that calculated from the analogy to thermal stress theory and FESA is reasonably achieved.

### References

- Abou-El-Leil, M. and Cooper, A.R.** (1978) Fracture of soda-lime glass tubes by field-assisted ion exchange, *J. Am. Ceram. Soc.* **61**: 131-136.
- Abou-El-Leil, M. and Cooper, A.R.** (1979) Analysis of field-assisted binary ion exchange, *J. Am. Ceram. Soc.* **62**: 390-395.

- Cooper, A.R. and Krohn, D.A.** (1969) Strengthening of glass fibers. II. Ion exchange, *J. Am. Ceram. Soc.* **52**: 665-669.
- Griffith, A.A.** (1920) Phenomena of rupture and flow in Solids, *Phil. Trans. Roy. Soc. London*, A **221**: 163-198; abstracted in *J. Am. Ceram. Soc.* (1921), **4**: 513.
- Holloway, D.G.** (1973) *The Physical Properties of Glass*, Wykeham publication, pp. 150-196.
- Hood, H.P. and Stookey, S.D.** (1961) Glass articles of high mechanical strength, *U.S. Pat.* 2, 998, 675.
- Krohn, D.A. and Cooper, A.R.** (1969) Strengthening of glass fibers. I. Cladding, *J. Am. Ceram. Soc.* **52**: 661-664.
- Ohta, H. and Hara, M.** (1970) Ion exchange in sheet glass by electrolysis, *Rep. Res. Lab. Asahi Glass Co., Ltd.* **20**: 15-32.
- Richmond, O., Leslie, W.C. and Wreidt, H.A.** (1964) Theory of residual stress due to chemical concentration gradient, *Trans. ASM* **57**: 294-300.
- Sane, A.Y. and Cooper, A.R.** (1978) Anomalous stress profiles in ion-exchanged glass, *J. Am. Ceram. Soc.* **61**: 359-362.
- Schaeffer, H.A. and Heinze, R.** (1974) Stress formation by ion exchange of glasses, *Glasstech. Ber.* **47**: 199-208.
- Shaisha, E.E. and Bahgat, A.A.** (1984) Stress relaxation in an ion exchanged glass, *Arab Gulf J. scient. Res.* **2**: 173-185.
- Shaisha, E.E. and Cooper, A.R.** (1981) Residual stress in singly and doubly ion-exchanged glass, *J. Am. Ceram. Soc.* **64**: 34-36.
- Wiederhorn, S.M.** (1975) Effect of zeta potential on crack propagation in glass, in aqueous solutions, *J. Am. Ceram. Soc.* **58**: 342-346.

(Received 04/10/1982;  
in revised form 30/05/1983)

## توزيع الإجهاد في حالة التبادل الأيوني في الزجاج

البيلي إسماعيل شعيشع ، علاء الدين عبد الحميد بهجت و

صلاح هاشم صلاح

قسم الطبيعة - كلية العلوم - جامعة الأزهر - مدينة نصر - القاهرة  
مصر

تمت دراسة توزيع الإجهاد الناتج عملياً من التبادل الأيوني للزجاج عند درجة حرارة  $350^{\circ}\text{C}$  ،  $500^{\circ}\text{C}$  وذلك بأخذ شرائح رقيقة جداً من الزجاج على هيئة حلقات دائرية وإجراء قياسات المرونة الضوئية لها ثم مقارنة النتائج العملية بكل من نظرية الإجهاد الحرارى وتحليل الإجهادات لعنصر صغير محدود باستخدام الحاسب الآلى . كما تمت الدراسة في حالة التبادل الأيوني في الاتجاه العكسى (وقد تم ذلك بعد إجراء تبادل أيوني على السطح الخارجى في اتجاه معين ثم عكس التيار الكهربى في الاتجاه الأخرى) ووجد أن الإجهاد في هذه الحالة يقل كثيراً عن المحسوب باستخدام نظرية الإجهاد الحرارى . كذلك تم تحليل نظرى لتوزيع الإجهادات باستخدام نظرية الإجهاد الحرارى .

كما تمت مناقشة توزيع الإجهادات باستخدام برنامج الحاسب الآلى لعنصر صغير محدود في بُعدين وكذلك التغير الذى يحدث في الإجهاد نتيجة تقسيم عينة الزجاج إلى شرائح صغيرة .